

Quantitative Assessment of Metabolic Flux by ^{13}C NMR Analysis. Biosynthesis of Anthraquinones in *Rubia tinctorum*

Dietmar Eichinger,[†] Adelbert Bacher,[†] Meinhart H. Zenk,[‡] and Wolfgang Eisenreich^{*,†}

Contribution from the Lehrstuhl für Organische Chemie und Biochemie, Technische Universität München, Lichtenbergstrasse 4, D-85747 Garching, Federal Republic of Germany, and Lehrstuhl für Pharmazeutische Biologie, Ludwigs-Maximilians-Universität München, Karlstrasse 29, D-80333 München, Federal Republic of Germany

Received February 26, 1999

Abstract: Cell cultures of the plant *Rubia tinctorum* were grown with supplements of $[1-^{13}\text{C}]$ - or $[\text{U}-^{13}\text{C}_6]$ -glucose. Amino acids were obtained by hydrolysis of biomass, and their ^{13}C labeling patterns were used to reconstruct the labeling patterns of acetyl CoA, pyruvate, phosphoenol pyruvate, erythrose 4-phosphate, and α -ketoglutarate by retrobiosynthetic analysis. These patterns were used to construct hypothetical labeling patterns for the anthraquinone, lucidin primveroside, via different hypothetical pathways. The predicted labeling pattern based on the precursors *o*-succinylbenzoate and dimethylallyl pyrophosphate derived via the deoxyxylulose pathway was in excellent agreement with the observed labeling pattern of the anthraquinone derivative. The data show that the retrobiosynthetic concept can be used to quantitatively estimate the flux of metabolites via different metabolic pathways.

Anthraquinone derivatives are found in microorganisms, fungi, plants, marine organisms, and insects. In higher plants, most anthraquinones occur as mono- or diglycosides. The yellow or red colored compounds have some commercial relevance as natural dyes. Moreover, 1,8-dihydroxyanthraquinones serve as laxatives.

In fungi and some higher plants (*Leguminosae*, *Rhamnaceae*, *Polygonaceae*, and *Caesalpiniaceae*), anthraquinones are biosynthesized via the polyketide pathway (Figure 1, pathway A).^{1–4} More specifically, successive condensation of acetyl CoA (1) with 7 molecules of malonyl CoA (2) provides an octa- β -keto-acyl chain (3) which is converted to the anthraquinone system such as emodin (4a) via decarboxylation, cyclization, and aromatization.

On the other hand, incorporation studies with radiolabeled shikimate (5), glutamate, and *o*-succinylbenzoate (8) suggested that *Rubiaceae* uses 8 derived from isochorismic acid (6) and α -ketoglutarate (7) as precursors for anthraquinone biosynthesis (Figure 1, pathway B).^{5–8} Cyclization of 8 was assumed to result in 1,4-dihydroxynaphthoic acid (9). Indirect support for this pathway was provided by the characterization of an enzyme from *Escherichia coli* catalyzing the formation of 8 from 7 and 6 but not from 7 and chorismic acid.⁹ Moreover, ^{13}C -labeled 8

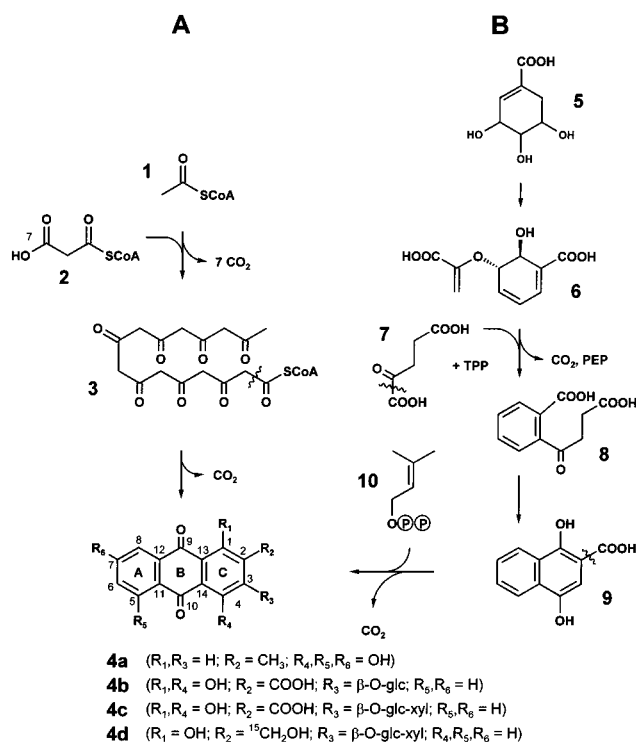


Figure 1. Pathways proposed in the literature for the biosynthesis of anthraquinones: (A) polyketide pathway^{1–4} and (B) *o*-succinylbenzoate/DMAPP pathway.^{5–13}

was shown to be incorporated into anthraquinones from cell cultures of the plant *Galium mollugo*.¹⁰

It was also shown that radiolabel from $[2-^{14}\text{C}]$ mevalonate is incorporated into the carboxylic group of purpurin-2-carboxylic acid 3-glucoside (4b), respectively purpurin-2-carboxylic acid

(10) Inoue, K.; Shiobara, Y.; Nayeshiro, H.; Inouye, H.; Wilson, G.; Zenk, M. H. *Phytochemistry* 1984, 23, 307–311.

* Address correspondence to this author.

[†] Technische Universität München.

[‡] Ludwigs-Maximilians-Universität München.

(1) Gatenbeck, S. *Acta Chem. Scand.* 1962, 16, 1053–1054.

(2) Leistner, E.; Zenk, M. H. *J. Chem. Soc., Chem. Commun.* 1969, 210–211.

(3) Paulick, R. C.; Casey, M. L.; Hillenbrand, D. F.; Whitlock, H. W. *J. Am. Chem. Soc.* 1975, 97, 5303–5305.

(4) Luckner, M. In *Secondary metabolism in microorganisms, plants and animals*, 3rd revised ed.; Springer-Verlag: New York, 1984; pp 176–178.

(5) Leistner, E.; Zenk, M. H. *Z. Naturforsch.* 1967, 22b, 865–868.

(6) Campbell, I. M. *Tetrahedron Lett.* 1969, 54, 4777–4780.

(7) Leistner, E. *Phytochemistry* 1973, 12a, 337–345.

(8) Leistner, E. *Phytochemistry* 1973, 12b, 1669–1674.

(9) Weische, A.; Leistner, E. *Tetrahedron Lett.* 1985, 26, 1487–1490.

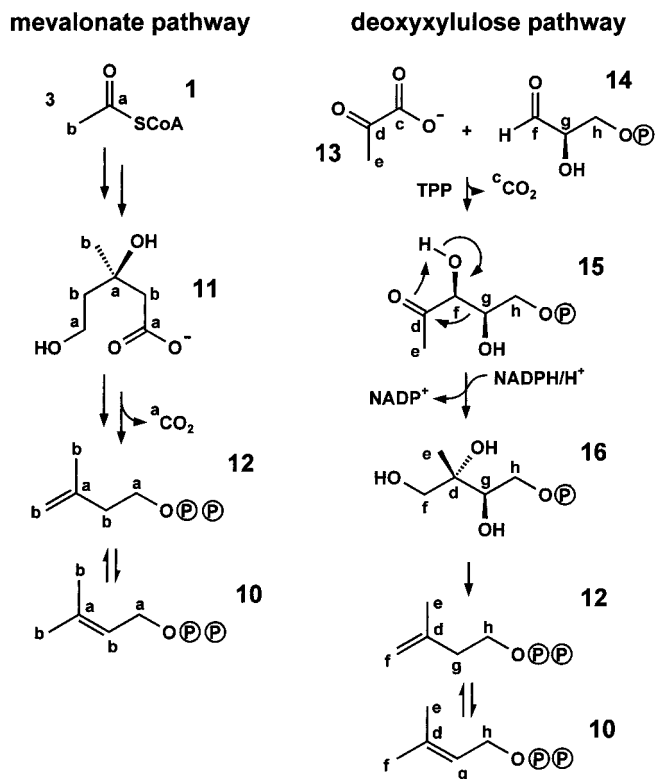


Figure 2. Diversion of carbon atoms from precursors to isoprenoid monomers by the mevalonate pathway and the deoxyxylulose pathway. The deoxyxylulose pathway involves a rearrangement of 1-deoxy-D-xylulose 5-phosphate (**15**) which interrupts the contiguity of the carbon atoms derived from the triose phosphate precursor.

3-primeveroside (**4c**) and other anthraquinones in *Rubia tinctorum*, albeit with very low incorporation rates (below 0.1%).^{7,11,12} In line with an earlier hypothesis by Sandermann and Dietrichs,¹³ this suggested that ring C of anthraquinones is derived from an isoprenoid precursor by condensation of **9** with dimethylallyl pyrophosphate (DMAPP, **10**) (Figure 1).

Despite conflicting observations, the mevalonate pathway (Figure 2) was considered for several decades as the unique pathway for isopentenyl pyrophosphate (IPP, **12**) and DMAPP (**10**) biosynthesis (for reviews see refs 14–16). However, recent studies by Rohmer, Sahn, Arigoni, Boronat, and their co-workers showed that many bacteria synthesize the building blocks of terpenoids by a different pathway starting from pyruvate (**13**) and glyceraldehyde 3-phosphate (**14**) via 1-deoxy-D-xylulose 5-phosphate (**15**) (Figure 2) (for reviews see refs 17 and 18). Arigoni, Schwarz, and Cartayrade discovered that this pathway is also operative in plants.^{19,20} On the other hand, several plants have been shown unequivocally to biosynthesize

Table 1. Isotope Incorporation Experiments with Cell Cultures of *Rubia tinctorum*^a

| ¹³ C-labeled precursor | concn [mM] | unlabeled glucose [mM] | culture vol [mL] |
|---|------------|------------------------|------------------|
| [U- ¹³ C ₆]glucose | 6.4 | 160.0 | 600 |
| [1- ¹³ C]glucose | 165.7 | 0 | 400 |

^a The precursors were added as a bolus at the beginning of the growth phase.

phytosterols and sesquiterpenes via mevalonate. The coexisting metabolic pathways appear to operate in different cell compartments. Specifically, the deoxyxylulose pathway operates in plastids, whereas the classical mevalonate pathway operates in the cytosol. However, at least one metabolite occurring in both pathways can be exchanged across compartment boundaries, since in *Salvia miltiorrhiza* plants and *Catharanthus roseus* cells sterols are formed from proffered 1-deoxy-D-xylulose to variable extents (0.5 and 6%, respectively) although the bulk of sterols are formed from mevalonate.^{20,21}

In light of these findings, the biosynthetic origin of individual terpenoids in plants cannot be assigned to one of the two terpenoid pathways by qualitative arguments; a quantitative analysis of metabolite flux through the competing pathways is required. This can be performed by the retrobiosynthetic concept illustrated in this paper in connection with studies on the biosynthesis of the anthraquinone, lucidin 3-primeveroside (**4d**, Figure 1), in a cell culture of *R. tinctorum*.

Experimental Section

Chemicals. [U-¹³C₆]- and [1-¹³C]glucose were purchased from Isotec (Miamisburg, OH).

Culture Medium. Suspension cultures of *R. tinctorum* were grown in LS medium²² and in B5 medium²³ containing 10 μM 2,4-dichlorophenoxyacetic acid. Sucrose was replaced by D-glucose (15 g per liter medium unless otherwise stated). The pH value of the medium was adjusted to 5.5 with 0.1 M NaOH prior to sterilization.

Cell Culture. Cells of *R. tinctorum* were grown in 250 mL Erlenmeyer flasks containing 130 mL of LS medium. After 7 days of growth, 60 mL of the cell suspension were added to 70 mL of B5 medium. The cultures were incubated on a rotary shaker (130 rpm) at 21 °C under a True Lite fluorescent tube (40W, Duro Lite Inc., Midland Park, NJ).

For isotope incorporation experiments, 5 g of wet cell mass grown for 7 days in B5 medium were suspended in 100 mL of B5 medium supplemented with 15 μM naphthylacetic acid. ¹³C-Labeled nutrients were added as sterile solutions (Table 1). After a growth period of 24 days, the cells were harvested, frozen in liquid nitrogen, and stored at -20 °C.

Isolation of Lucidin 3-Primeveroside (4d). Wet cells of *R. tinctorum* (120 g) were suspended in 200 mL of water and homogenized with an Ultra Turrax mixer (20000 U/min, 5 min). The mixture was freeze-dried (7.4 g) and extracted for 24 h with 600 mL of methanol at 65 °C using a Soxhlet extractor. The extract was concentrated to dryness under reduced pressure and the residue was dissolved in 150 mL of water. The solution was continuously extracted with 300 mL of diethyl ether for 12 h using a liquid/liquid perforator. The aqueous solution was saturated with sodium chloride and then extracted with *n*-butanol (4 × 100 mL). The organic phases were combined and concentrated to dryness under reduced pressure. The residue was triturated with a mixture of methanol/water (v/v, 1:9, 200 mL), and insoluble material was removed by centrifugation (15 min, 7500 U/min, 4 °C). The supernatant was applied to a column of Amberlite XAD-2 (3.2 × 17 cm) which was subsequently washed with 1.5 L of 30% (v/v) aqueous

(11) Leistner, E.; Zenk, M. H. *Tetrahedron Lett.* **1968**, *11*, 1395–1396.

(12) Burnett, A. R.; Thomson, R. H. *J. Chem. Soc. C* **1968**, *17*, 2437–2441.

(13) Sandermann, W.; Dietrichs, H. H. *Holzforchung* **1959**, *13*, 137–148.

(14) Qureshi, N.; Porter, J. W. In *Biosynthesis of isoprenoid compounds*; Porter, J. W.; Spurgeon, S. L., Eds.; John Wiley: New York, 1981; Vol. 1, pp 47–94.

(15) Bloch, K. *Steroids* **1992**, *57*, 378–382.

(16) Bach, T. J. *Lipids* **1995**, *30*, 191–202.

(17) Rohmer, M. *Prog. Drug. Res.* **1998**, *50*, 135–154.

(18) Eisenreich, W.; Schwarz, M.; Cartayrade, A.; Arigoni, D.; Zenk, M. H.; Bacher, A. *Chem. Biol.* **1998**, *5*, 221–233.

(19) Schwarz, M. K. Thesis No. 10951, 1994, ETH Zürich, Switzerland.

(20) Cartayrade, A.; Schwarz, M. K.; Jaun, B.; Arigoni, D. Second Symposium of the European Network on Plant Terpenoids, Strasbourg/Bischenberg, Jan. 23–27, 1994, Abstract P1.

(21) Arigoni, D.; Sagner, S.; Latzel, C.; Eisenreich, W.; Bacher, A.; Zenk, M. H. *Proc. Natl. Acad. Sci. U.S.A.* **1997**, *94*, 10600–10605.

(22) Linsmaier, E. M.; Skoog, F. *Physiol. Plant.* **1965**, *18*, 100–127.

(23) Gamborg, O. L.; Miller, R. A.; Ojima, K. *Exp. Cell Res.* **1968**, *50*, 151–158.

Table 2. ^1H and ^{13}C NMR Signal Assignments of Lucidin 3-Primeveroside

| position | chemical shifts, ppm | | coupling constants, Hz | | DQF-COSY | INADEQUATE | ^{13}C -TOCSY |
|----------|-------------------------|--------------|------------------------|----------------------|---------------|------------|------------------------|
| | ^{13}C | ^1H | J_{CC}^a | J_{HH} | | | |
| 1 | 162.2 (C) | | 69.2 (2) | | | 2 | 2 |
| 2 | 124.0 (C) | | 69.2 (1), 47.9 (15) | | | 1,15 | 1 |
| 3 | 162.4 (C) | | 65.1 (4) | | | 4 | 4 |
| 4 | 106.8 (CH) | 7.43 (d) | 65.1 (3) | 1.2 (15) | | 3 | 3 |
| 5 | 127.3 (CH) | 8.18 (m) | 59.5 (11), 55.9 (6) | | 6 | 11 | |
| 6 | 135.3 (CH) | 8.13 (m) | 55.5 (5) | | 5,7 | | |
| 7 | 135.1 (CH) | 8.13 (m) | | | 6,8 | | |
| 8 | 126.9 (CH) | 8.18 (m) | 59.5 (12) | | 7 | 12 | 9,12 |
| 9 | 187.5 (C) | | 54.4 (12) | | | 12 | 8,12 |
| 10 | 181.9 (C) | | 54.0 (14) | | | 14 | 14 |
| 11 | 133.3 (C) | | 59.6 (5) | | | 5 | |
| 12 | 133.2 (C) | | 59.5 (8), 54.3 (9) | | | 8,9 | 8,9 |
| 13 | 111.8 (C) | | 56.7 (14) | | | | |
| 14 | 134.2 (C) | | 54.0 (10) | | | 10 | 10 |
| 1' | 101.2 (CH) | 5.08 (d) | 46.6 (2') | 7.4 (2') | 2' | 2' | 2',3',4',5',6' |
| 2' | 73.7 (CH) | 3.37 (m) | 46.4 (1') | | 1',3' | 1',3' | 1',3',4',5',6' |
| 3' | 76.2 (CH) | 3.35 (m) | | | 2',4' | 2' | 1',2',4',5' |
| 4' | 69.5 (CH) | 3.32 (m) | 41.0 (5') | | 3',5' | 5' | 1',2',3',5',6' |
| 5' | 76.1 (CH) | 3.62 (m) | | | 4',6'a,6'b | 6' | 1',2',3',4',6' |
| 6'a | 68.4 (CH ₂) | 3.94 (dd) | 44.8 (5') | 11.3 (6'b), 1.5 (5') | 5',6'b | 5' | 1',2',3',4',5' |
| 6'b | | 3.65 (m) | | | 5',6'a | 5' | 1',2',3',4',5' |
| 1'' | 104.4 (CH) | 4.11 (d) | 46.8 (2''), 4.2 (3'') | 7.5 (2'') | 2'' | 2'' | 2'',3'',4'',5'' |
| 2'' | 73.8 (CH) | 2.99 (m) | 46.8 (1'') | | 1'',3'' | 1'',3'' | 1'',3'',4'',5'' |
| 3'' | 76.8 (CH) | 3.06 (t) | | 8.7 (2'',4'') | 2'',4'' | 2'' | 1'',2'',4'',5'' |
| 4'' | 69.8 (CH) | 3.29 (m) | 40.2 (5'') | | 3'',5''a,5''b | 5'' | 1'',2'',3'',5'' |
| 5''a | 66.0 (CH ₂) | 3.68 (m) | 40.2 (4'') | | 4'',5''b | 4'' | 1'',2'',3'',4'' |
| 5''b | | 2.99 (m) | | | 4'',5''a | 4'' | 1'',2'',3'',4'' |
| 15a | 51.3 (CH ₂) | 4.61 (dd) | 47.5 (2) | 11.2 (15b), 1.1 (4) | 15a | 2 | |
| 15b | | 4.53 (d) | | 11.2 (15a) | 15b | 2 | |

^a ^{13}C - ^{13}C coupling constants obtained from a one-dimensional ^{13}C NMR spectrum of a sample obtained from the experiment with $[\text{U-}^{13}\text{C}_6]\text{glucose}$. Carbon atoms coupled to the respective index carbon are in parentheses and were determined by INADEQUATE spectroscopy.

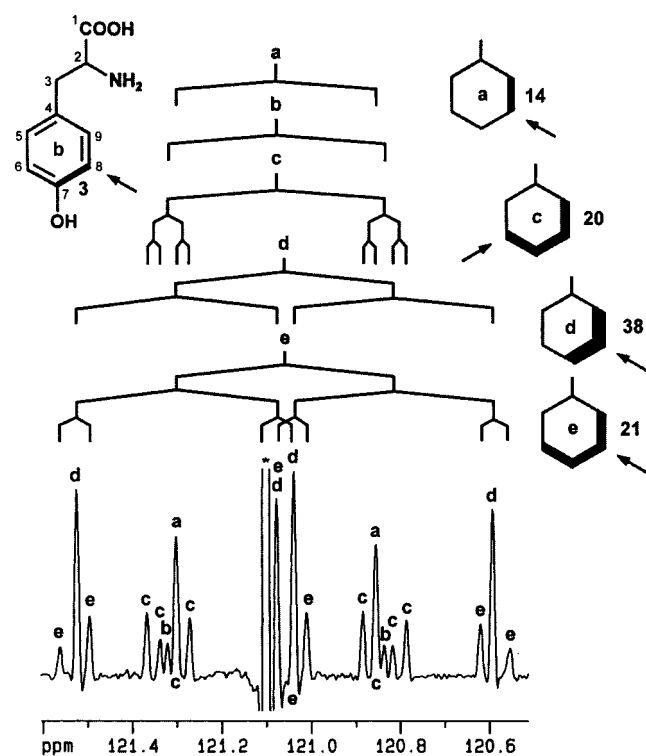


Figure 3. ^1H -decoupled ^{13}C NMR signals of C-6/8 of tyrosine from *R. tinctorum* after incorporation of $[\text{U-}^{13}\text{C}_6]\text{glucose}$ diluted with unlabeled glucose (1:24, w/w). The asterisk indicates natural abundance background (truncated). The respective tyrosine isotopomers a–e are shown schematically with bold lines connecting adjacent ^{13}C atoms. The observed carbon is marked by an arrow. The numbers indicate isotopomer ratios normalized to the global signal intensity, arbitrarily set to 100.

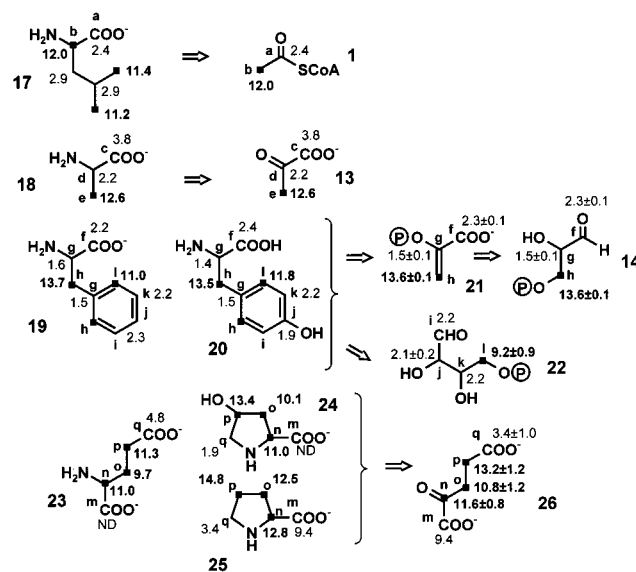


Figure 4. ^{13}C abundances (in % ^{13}C) of amino acids from *R. tinctorum* after incorporation of $[\text{1-}^{13}\text{C}]\text{glucose}$. The reconstruction of the labeling patterns of central metabolic intermediates is based on established mechanisms and is indicated by the symbol \Rightarrow .

methanol. Compound **4d** was eluted with 2.0 L of 50% aqueous methanol (v/v). The effluent was concentrated under reduced pressure. The residue was dissolved in 10 mL of methanol.

Crude **4d** was purified by preparative reversed-phase HPLC using a column of Nucleosil RP18 (16 \times 250 mm). The column was developed with 50% aqueous methanol (flow rate, 8 mL/min). The effluent was monitored photometrically (254 nm; retention volume of **4d**, 100 mL). Fractions were combined and concentrated to dryness under reduced pressure.

Isolation of Amino Acids. Methanol-extracted cell mass was treated with 150 mL of 6 M HCl containing 0.5 M thioglycolic acid for 24 h

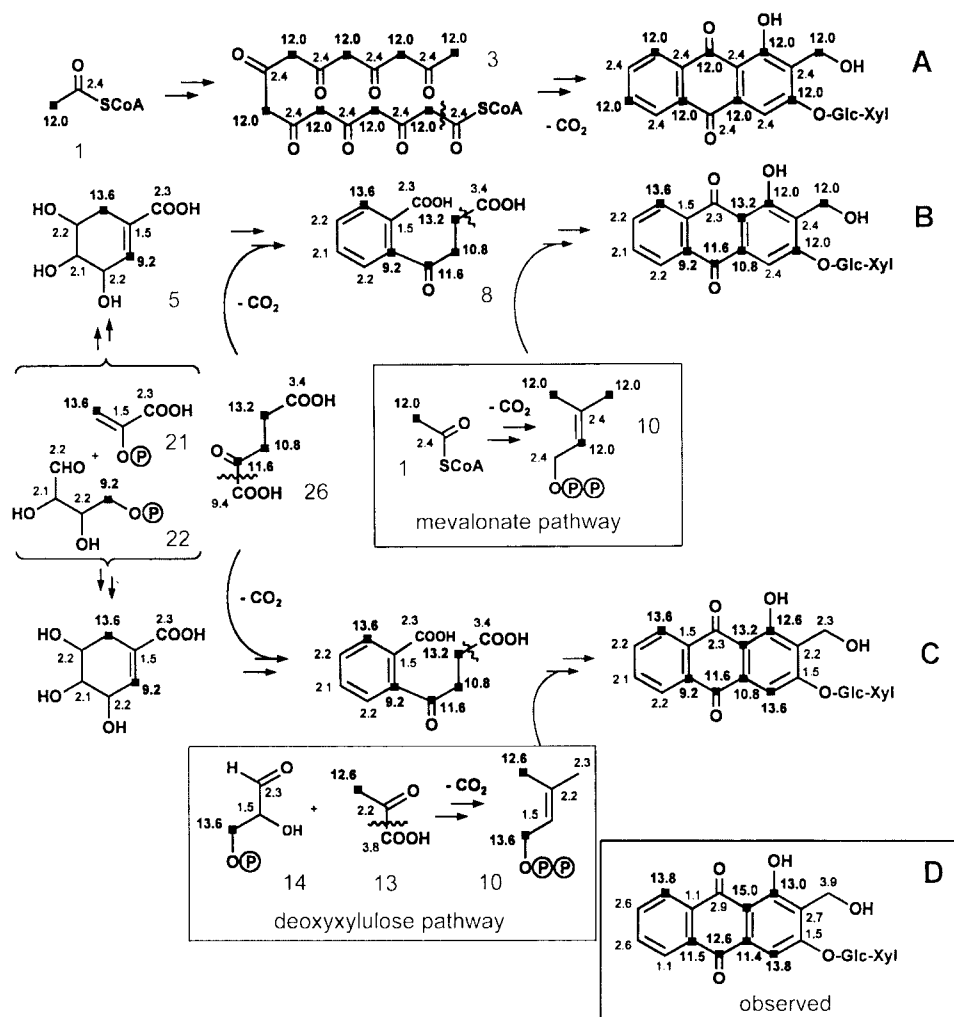


Figure 5. Labeling patterns in lucidin 3-primeveroside and central metabolites after feeding of [$1\text{-}^{13}\text{C}$]glucose to cell cultures of *R. tinctorum*. The numbers indicate ^{13}C abundance in % ^{13}C . The squares indicate significantly ^{13}C enriched positions. (A) The labeling pattern of the octa- β -ketoacyl compound (**3**, polyketid pathway) was predicted on the basis of the labeling data from acetyl CoA (**1**) (see Figure 4). (B and C) The labeling pattern of shikimic acid (**5**) was predicted on the basis of the labeling data of erythrose 4-phosphate (**22**) and phosphoenol pyruvate (**21**) (*o*-succinylbenzoate/DMAPP pathway). Predictions of the labeling patterns of DMAPP (**10**) were made on basis of the labeling data of acetyl-CoA (**1**) (B, mevalonate pathway) or pyruvate (**13**) and glyceraldehyde 3-phosphate (**14**) (C, deoxyxylulose pathway), as reconstructed from amino acids (see Figure 4). (D) Observed labeling pattern.

at 120 °C. The mixture was filtered, and the supernatant was evaporated to dryness. The mixture was filtered, and the supernatant was evaporated to dryness. Amino acids were isolated from the residue as described earlier.²⁴

NMR Spectroscopy. ^1H and ^{13}C NMR spectra were recorded at 500 and 125 MHz, respectively, using a Bruker DRX 500 spectrometer. One-dimensional and two-dimensional experiments (DQF-COSY, INADEQUATE, and ^{13}C TOCSY) were performed at 27 °C using standard Bruker software (XWINNMR 1.3). Compound **4d** was measured in DMSO- d_6 as solvent. Amino acids were measured in D_2O at pH 1 or 13. ^1H and ^{13}C coupling patterns were simulated with the program package NMRSIM (Bruker).

Results

NMR Signal Assignment. The correct interpretation of ^{13}C labeling experiments by quantitative NMR spectroscopy requires unequivocal assignments of ^1H and ^{13}C NMR signals. A comprehensive NMR analysis of lucidin 3-primeveroside (**4d**) was performed by two-dimensional homo- and heterocorrelation experiments. $^{13}\text{C}^{13}\text{C}$ couplings in **4d** from the incorporation experiment with [$U\text{-}^{13}\text{C}_6$]glucose gave additional confirmation (Table 2).

Isotope Incorporation Studies. Cells of *R. tinctorum* were grown in medium containing [$1\text{-}^{13}\text{C}$]glucose or a mixture of [$U\text{-}^{13}\text{C}_6$]glucose and unlabeled glucose (1:24; w/w) as the sole carbon source. Compound **4d** was isolated in amounts of about 6 mg per g of cell mass (dry weight). ^{13}C Isotopomer compositions of **4d** and of amino acids isolated from cellular protein were determined by quantitative ^{13}C NMR spectroscopy.²⁵

In the experiment with [$U\text{-}^{13}\text{C}_6$]glucose, the labeled precursor was proffered together with a 24-fold excess of unlabeled glucose. This feeding strategy is conducive to the formation of downstream metabolites by random combination of metabolic intermediates derived from multiple ^{13}C -labeled and unlabeled glucose molecules, respectively. The resulting metabolites are mixtures of numerous singly or multiply ^{13}C -labeled isotopomers. Most of the ^{13}C NMR signals therefore appear as complex multiplets which result from $^{13}\text{C}^{13}\text{C}$ couplings and reflect the various multiple ^{13}C -labeled isotopomers in the mixture. As an example, the complex ^{13}C NMR signature of C-6/C-8 of tyrosine isolated from the *R. tinctorum* cell culture

(24) Eisenreich, W.; Schwarzkopf, B.; Bacher, A. *J. Biol. Chem.* **1991**, 266, 9622–9631.

(25) Werner, I.; Bacher, A.; Eisenreich, W. *J. Biol. Chem.* **1997**, 272, 25474–25482.

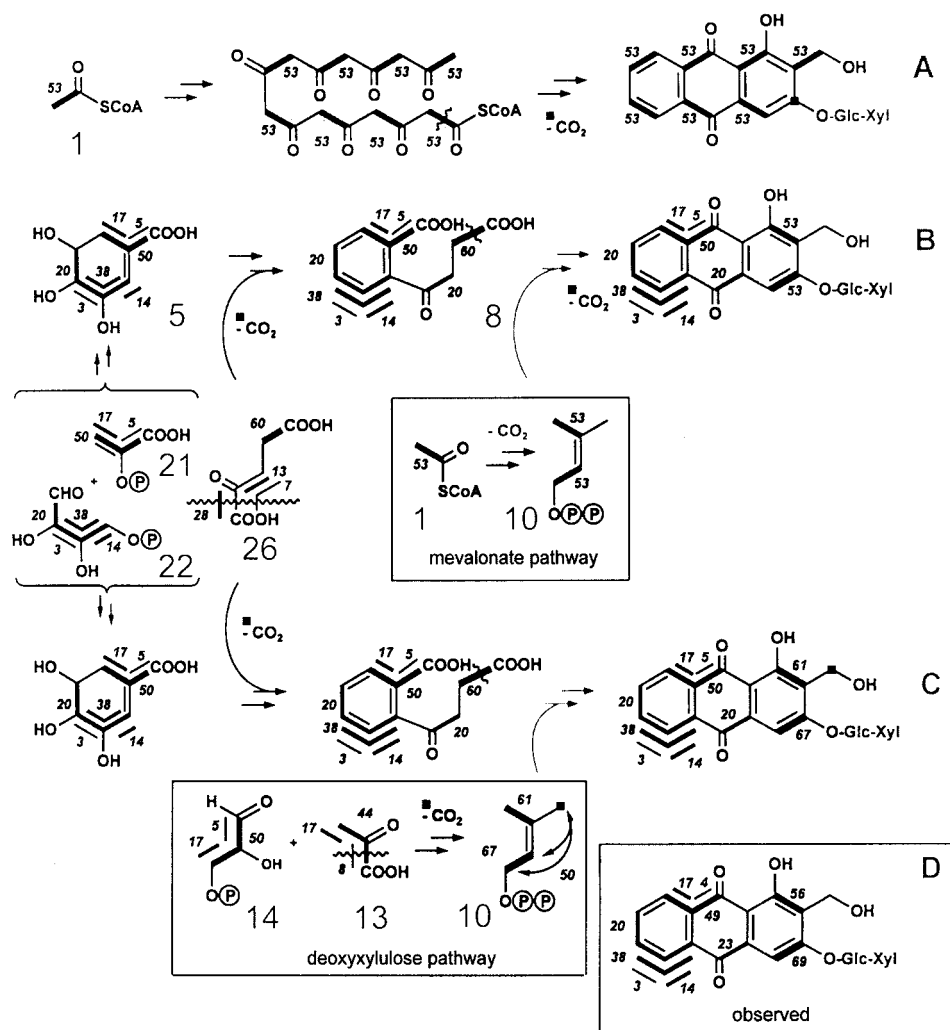


Figure 6. Labeling patterns of lucidin 3-primeveroside and central metabolites after feeding of $[\text{U-}^{13}\text{C}_6]$ glucose diluted with unlabeled glucose (1:24, w/w) to cell cultures of *R. tinctorum*. Contiguous ^{13}C labeled isotopomers are indicated by bold lines connecting ^{13}C atoms. The numbers indicate isotopomer ratios normalized to the global ^{13}C NMR signal intensity of the respective carbon atom, arbitrarily set to 100. For further details see Figure 5.

is shown in Figure 3. The truncated signal marked by an asterisk represents tyrosine with a single ^{13}C atom in position 6 or 8, which is predominantly formed from the natural abundance glucose. The satellite signals are caused by $^{13}\text{C}^{13}\text{C}$ coupling and represent multiple ^{13}C -labeled isotopomers reflecting biosynthetic contributions from the totally ^{13}C -labeled glucose. These isotopomers were assessed by deconvolution of the $^{13}\text{C}^{13}\text{C}$ coupling multiplets as described earlier.²⁵ The fraction of each isotopomer in the mixture can be determined by integration of the signal components representing each individual isotopomer. Some isotopomers can be estimated from more than one spectral pattern. As an example, different coupling patterns were detected for $[\text{5,6,7,8-}^{13}\text{C}_4]$ tyrosine in the signature of C-6/C-8 of tyrosine and the abundance of $[\text{5,6,7,8-}^{13}\text{C}_4]$ tyrosine could be determined independently from the signals of isotopomer c (20.2% relative abundance) and isotopomer e (20.8% relative abundance) (Figure 3). Moreover, the abundance of $[\text{5,6,7,8-}^{13}\text{C}_4]$ tyrosine as determined from the signal of C-7 of tyrosine (20.3% relative abundance) was in good agreement demonstrating the accuracy of the experimental protocol.

Reconstruction of Labeling Patterns for Central Metabolites. As described in detail elsewhere,^{25–28} the labeling patterns

of amino acids can be used to reconstruct the labeling patterns of central intermediates which cannot be analyzed directly in consequence of their relatively low abundance in biomass. Thus, the labeling pattern of acetyl CoA (1) can be gleaned from carbon atoms a and b of leucine (17, Figure 4). The labeling pattern of pyruvate (13) is determined from that of alanine (18). The labeling pattern of glyceraldehyde 3-phosphate (14) resembles that of phosphoenol pyruvate (21), which is accessible via the side chains of phenylalanine (19) and tyrosine (20). The labeling pattern of α -ketoglutarate (26) is reflected in glutamate (23), 4-hydroxyproline (24), and proline (25). The labeling pattern of erythrose 4-phosphate (22) can be reconstructed from the aromatic rings of phenylalanine (19) and tyrosine (20). Although it should be noted that the contributions by erythrose 4-phosphate (22) and phosphoenol pyruvate (21) to the atoms l and h of the aromatic amino acids become averaged by the symmetry of the benzenoid ring, the contribution of 22 can be calculated from the known labeling pattern of 21 (see above).

Prediction of Labeling Patterns via Different Pathways. The deduced labeling patterns of the central metabolic intermediates were used to quantitatively predict the diversion of

(27) Eichinger, D.; Bacher, A.; Zenk, M. H.; Eisenreich, W. *Phytochemistry* **1999**, *51*, 223–236.

(28) Rieder, C.; Strauss, G.; Fuchs, G.; Arigoni, D.; Bacher, A.; Eisenreich, W. *J. Biol. Chem.* **1998**, *273*, 18099–18108.

(26) Bacher, A.; Rieder, C.; Eichinger, D.; Arigoni, D.; Fuchs, G.; Eisenreich, W. *FEMS Microbiol. Rev.* **1999**, *22*, 567–598.

isotope to **4d** via different hypothetical pathways (Figures 5 and 6). These simulations considered three different working models, i.e., a polyketide origin of the entire ring system (prediction A), a shikimate origin of ring A (prediction B, C), a mevalonate origin of ring C (prediction B), and a deoxyxylulose origin of ring C (prediction C).

The observed ^{13}C labeling patterns (D, Figures 5 and 6) in lucidin 3-primeveroside cannot be accommodated with a biogenesis via a polyketide mechanism (A, Figures 5 and 6), and a biosynthesis of the anthraquinone system via an octa- β -ketoacyl chain (**3**) can thus be clearly ruled out. On the other hand, the observed labeling patterns in ring A of **4d** are in almost perfect agreement with the predicted labeling patterns of shikimate (**5**). Similarly, the carbon atoms 10, 14, and 13 of lucidin 3-primeveroside show close correspondence with carbon atoms 2, 3, and 4 of α -ketoglutarate (**26**). Thus, the data leave no doubt that ring A and ring B of **4d** stem from the carbon skeleton of shikimic acid (**5**) and α -ketoglutarate (**26**) via *o*-succinylbenzoate (**8**), respectively.

The following features of the experimentally observed labeling pattern in **4d** (D, Figure 6) isolated from the experiment with $[\text{U-}^{13}\text{C}_6]\text{glucose}$ deserve particular interest. The presence of $[8,12,9\text{-}^{13}\text{C}_3]\text{4d}$ in the biosynthetic isotopomer mixture was evident from the one-dimensional ^{13}C NMR spectrum as well as from two-dimensional INADEQUATE experiments. This isotopomer as well as the $[8,12\text{-}^{13}\text{C}_2]$ - and $[12,9\text{-}^{13}\text{C}_2]$ -isotopomers reflect perfectly the predicted isotopomer composition of shikimate (**5**) where the respective 3-carbon moiety is derived from phosphoenol pyruvate (**21**) (Figure 6). The NMR signals of C-6 and C-7 of **4d** show non-first-order ^{13}C couplings (D, Figure 7) which were simulated using the numerical data in the labeling predictions in Figure 6A (polyketide pathway) and Figure 6B (via shikimate). The observed signal pattern in biosynthetic anthraquinone (D, Figure 7) is in excellent agreement with the shikimate prediction (C, Figure 7), but not with the polyketide prediction (B, Figure 7).

Of special interest is the biosynthetic origin of DMAPP (**10**) used for the formation of ring C in lucidin 3-primeveroside. The hypothetical labeling pattern expected for the formation of isoprenoid C_5 units via mevalonate is easily predicted from the labeling pattern of acetyl CoA (**1**). On the other hand, the hypothetical pattern obtained via the deoxyxylulose pathway can be predicted from the reconstructed labeling patterns of glyceraldehyde 3-phosphate (**14**) and pyruvate (**13**).

In the experiment with $[1\text{-}^{13}\text{C}]\text{glucose}$, the mevalonate resp. deoxyxylulose prediction resulted in characteristic patterns with high ^{13}C abundances in C-1 and C-4 of **4d** via the deoxyxylulose pathway (C, Figure 5), and C-1, C-3, and C-15 of **4d** via the mevalonate route (B, Figure 5). The observed labeling pattern of the isoprenoid moiety in **4d** (D, Figure 5) closely resembles the predicted pattern via **13** and **14** demonstrating that the terpenoid block of lucidin 3-primeveroside predominantly originates via 1-deoxy-D-xylulose 5-phosphate.

Discussion

Tracer studies with radioactive or stable isotopes are important and time-honored tools for the elucidation of metabolic pathways. Usually, the experimental data are interpreted in a qualitative fashion. The diversion of isotope from a given isotope-labeled compound to a downstream metabolite is taken as evidence for its role as a precursor. This approach overlooks that the diversion of isotope to a target can in principle occur by different routes affording more or less extensive reshuffling in intermediary metabolism rather than by a direct biosynthetic route.

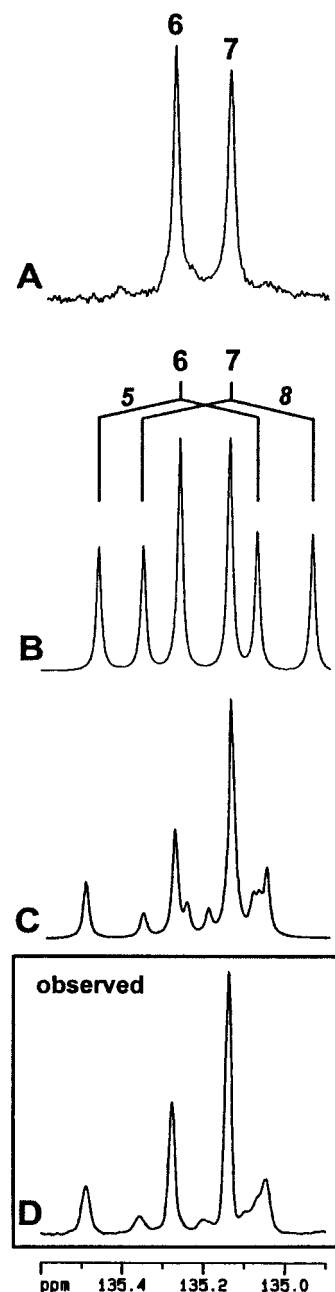


Figure 7. Observed and simulated ^{13}C NMR signatures of C-6 and C-7 of lucidin 3-primeveroside after feeding of $[\text{U-}^{13}\text{C}_6]\text{glucose}$ diluted with unlabeled glucose (1:24, w/w) to cell cultures of *R. tinctorum*. (A) Observed signals of a natural ^{13}C abundance sample; (B) simulation via the polyketide pathway; (C) simulation via the *o*-succinylbenzoate pathway; and (D) observed signals of the sample from the experiment with $[\text{U-}^{13}\text{C}_6]\text{glucose}$.

The biosynthesis of terpenoids is replete with examples illustrating these pitfalls. Since the discovery of the mevalonate pathway of isoprenoid biosynthesis by the pioneering work of Bloch, Lynen, and Cornforth (for reviews see refs 14–16) mevalonate and acetate have been used in numerous studies to document the biosynthetic origin of terpenoids in microorganisms, plants, and animals. Even the diversion of tiny fractions of radiolabeled mevalonate was then accepted as evidence for the mevalonate origin of the target compound. This appeared as an undisputable approach at least in those cases where the investigators took the trouble to monitor the specific positions of the incorporated radiolabel in the target metabolite by painstaking chemical degradation.

Recently, an alternative pathway to plant isoprenoids via 1-deoxyxylulose 5-phosphate has been discovered.^{19,20} It is now well established that numerous monoterpenes, diterpenes, and tetraterpenes are biosynthesized via the deoxyxylulose pathway in plants,^{18,17} whereas phytosterols are biosynthesized by the classical mevalonate pathway. Specifically, the mevalonate pathway appears to proceed in the cytoplasm, and the deoxyxylulose pathway appears to be operative in plastids.^{21,29}

The experimental labeling patterns in lucidin primeveroside obtained from [1-¹³C]glucose or from a mixture of [U-¹³C₆]glucose and unlabeled glucose agree well with the predictions of the *o*-succinylbenzoate pathway of anthraquinone biosynthesis and the deoxyxylulose pathway of IPP/DMAPP biosynthesis. More specifically, the data indicate that more than 95% of the terpenoid precursor of ring C has been contributed via the deoxyxylulose pathway. This strongly suggests that the condensation of 1,4-dihydroxynaphthoic acid (**9**) with DMAPP (**10**) occurs in the plastid compartment of the plant cell.

A series of recent studies used isotope-labeled 1-deoxy-D-xylulose to establish the deoxyxylulose origin of various

terpenoids in a variety of plant species (for review see ref 17). Many of these studies are fraught with the same problems as the earlier mevalonate studies. Unless the incorporation rates are very high, the incorporation of 1-deoxy-D-xylulose into a given plant metabolite cannot serve as proof for a predominant deoxyxylulose origin. As a consequence of the crosstalk between the two pathways, some incorporations of 1-deoxy-D-xylulose would be observed even if mevalonate served as the mainstream contributor to a given metabolite.

To establish the predominant origin of a given terpenoid in plants, it is mandatory to use methods which can address metabolic flux patterns quantitatively rather than qualitatively. The retrobiosynthetic approach used in this study affords quantitative predictions of labeling patterns for each of the pathways based on the labeling patterns of central metabolic intermediates reconstructed from the labeling pattern of primary metabolites.

Acknowledgment. This work was supported by the Deutsche Forschungsgemeinschaft (SFB 369) and the Fonds der Chemischen Industrie. We thank Angelika Werner and Fritz Wendling for expert help with the preparation of the manuscript.

JA990622O

(29) Schwender, J.; Zeidler, J.; Gröner, R.; Müller, C.; Focke, M.; Braun, S.; Lichtenthaler, F. W.; Lichtenthaler, H. K. *FEBS Lett.* **1997**, *414*, 129–134.